

# Deepening mechanisms of cut-off lows in the Southern Hemisphere and the role of jet streams: insights from eddy kinetic energy analysis

## ~~Exploring the vertical extent and deepening mechanisms of cut-off lows in the Southern Hemisphere: insights from eddy kinetic energy analysis~~

Henri R. Pinheiro<sup>1</sup>, Kevin I. Hodges<sup>2</sup>, Manoel A. Gan<sup>3</sup>

<sup>1</sup>Department of Atmospheric Sciences, University of Sao Paulo, 05508-090, Brazil.

<sup>2</sup>Department of Meteorology, University of Reading, Reading, RG6 6UR, United Kingdom.

<sup>3</sup>Center for Weather Forecast and Climate Studies (CPTEC), National Institute for Space Research (INPE), Sao Jose dos Campos, 12227-010, Brazil.

Correspondence to: Kevin I. Hodges ([k.i.hodges@reading.ac.uk](mailto:k.i.hodges@reading.ac.uk))

**Abstract.** Cut-off lows (COLs) exhibit diverse structures and lifecycles, ranging from confined upper tropospheric systems to deep, multi-level vortex structures. While COL climatologies are well-documented, the mechanisms driving their deepening remain unclear. To bridge this gap, a novel track matching algorithm applied to ERA-Interim reanalysis investigates the vertical extent of Southern Hemisphere COLs. Composite analysis based on structure and eddy kinetic energy budget differentiates four COL categories: shallow, deep, weak, and strong, revealing similarities and disparities. Deep, strong COLs concentrate around Australia and the southwestern Pacific, peaking in autumn and spring, while shallow, weak COLs are more common in summer and closer to the equator. Despite differences, both contrasting types evolve energetically via anticyclonic Rossby wave breaking. The distinct roles of jet streams in affecting COL types: intense polar front jet correlates with more deep COLs, whereas stronger subtropical jet relates to fewer shallow COLs. Deepening mechanisms involve eddy feedback between upper and lower tropospheric systems, induced by an intense upstream poleward jet enhancing ageostrophic flux convergence behind the COLs, accompanied by baroclinic processes flanking the COLs. Additionally, we highlight the significance of diabatic processes in COL deepening, addressing their misrepresentation in reanalysis and emphasizing the need for more observational and modelling studies to refine the energetic framework.

**Keywords:** Cut-off Lows, Vertical Depth, ~~Extensions~~, Deepening, Jet Streams, Energetics, Eddy Kinetic Energy.

## 1 Introduction

30 Cut-off low (COL) pressure systems are ~~characterized by~~ closed low-pressure ~~centers systems~~ that detach or ~~are~~ "cut-off" from the main westerly flow (Palmén 1949). ~~These systems manifest as isolated cyclonic potential vorticity anomalies~~ ~~Typically forming and form both~~ equatorward ~~and poleward from of the~~ polar front or mid-latitude jet (Portmann et al. 2021). ~~they can be identified as isolated high potential vorticity anomalies~~. COLs are known for their slow movement, varying in duration from short-lived to persisting for several days. ~~Their Prolonged-prolonged~~ periods of precipitation associated with COLs often result in significant accumulations and ~~may lead to eventually~~ floods in various locations (Singleton and Reason 20062007, Llasat et al. 2007, ~~McInessMcInnes~~ and Hubbert 2011)

~~The vertical extent and deepening mechanisms in cut-off low (COLs) pressure systems represent important research topics in weather and climate research. Understanding the key aspects of the vertical extent and mechanisms that deepen COLs is of great importance because it offers valuable insights into the dynamics and evolution of these systems. Moreover, such understanding is crucial for enhancing the accuracy of COL prediction.~~

40 ~~One critical aspect of COLs is their vertical extent, which directly influences their precipitation intensity and duration. Deep COLs, reaching lower atmospheric levels, are usually linked to heavier rainfall compared to shallow systems (Porcù et al. 2007, Pinheiro et al. 2021). Early studies (Palmén 1979) established a groundwork for understanding their vertical structure. A seminal work to address the vertical structure of COLs is that of Palmén (1949) which revealed-revealing their key~~ features of these systems such as ~~the a~~ quasi-barotropic structure, tropopause folding and thermal dipole patterns ~~associated with cold and warm cores~~. ~~Later~~Subsequent studies, including those of Frank (1970) and Porcù et al. (2007), observed ~~that a~~ clear relationship exists between ~~the COL~~ vertical extent of COLs and the associated cloud and precipitation patterns, ~~which was corroborated by a more recent observational study (Porcù et al. 2007)~~. More recently, Portmann et al. (2021) highlighted the influence of jet streams on the precipitation intensity of COLs based on their relative position.

50 ~~The vertical depth of COLs plays a critical role in determining weather conditions, directly influencing the intensity, duration and spatial extent of precipitation. In particular, deep COLs often lead to more intense precipitation and higher accumulations compared to their shallow counterparts (Porcù et al. 2007; Pinheiro et al. 2021).~~

~~Nevertheless, the current literature lacks comprehensive studies addressing the potential mechanisms involved in the deepening of COLs. Analyzing the development of atmospheric systems from an energy perspective offers valuable insights into the diverse processes and interactions, including the various forms of generation, conversion and redistribution of kinetic energy.~~

55 ~~Recently, there have been s~~Significant ~~advances progress has been made~~ in the understanding of the mechanisms underlying driving the development of COLs. ~~Notably, studies- Studies~~ have shed light on the crucial role ~~of played by the mid-latitude~~

jet streams in supplying energy to ~~COLs these systems~~ (Pinto and Rocha 2011; Gan and Piva 2013; Ndarana et al. 2021).  
60 particularly in regions of high topography such as the Andes Cordillera in South America (Gan and Dal Piva 2016; Pinheiro  
et al. 2021) and the southern African plateau (Ndarana et al. 2021). Split jet streams Their formation often results from a  
split flow associated with Rossby wave breaking, leading to convergence of ageostrophic geopotential fluxes (hereafter,  
ageostrophic fluxes) and baroclinic processes. Rossby wave breaking facilitate the transfer of eddy kinetic energy (EKE)  
from the mid-latitude jet into the circulation of the COL, thereby intensifying the system (Ndarana et al. 2021, Pinheiro et  
65 al. 2022). The impact of ageostrophic fluxes on COLs is twofold: convergence enhances the development, while divergence  
promotes decay. Baroclinic processes, especially within intense COLs, have been identified as the primary source of kinetic  
energy (Pinheiro et al. 2021). Furthermore, the energy budget is influenced by ~~d~~Diabatic processes, such as radiative cooling  
and latent heating, also play a role in COL development, as demonstrated by various studies (Sakamoto and Takahashi 2005;  
Garreaud and Fuenzalida 2007, Cavallo and Hakim 2010, Portmann et al. 2018). Additionally, the interaction between  
70 upper-level potential vorticity and low-level potential temperature anomalies has emerged as a crucial mechanism  
influencing the extent of COLs (Barnes et al. 2021).

Despite these advancements, a comprehensive understanding of COL deepening mechanisms remains unclear. The role of jet  
streams in deepening COLs and the complex influence of diabatic processes require further investigation. Elucidating these  
key aspects is crucial for both accurate predictions and improved understanding of COL dynamics. This study aims to  
75 provide an explanation for the deepening of COLs address these critical gaps by employing energetic diagnostics. A novel  
approach is introduced to determine the vertical depth of COLs, followed by the application of the local EKE budget. These  
techniques present an opportunity to address by addressing the following scientific questions:

1. How sensitive are methods used to determine the for estimating the vertical depth of COLs?

4.2. Can COLs be affectively classified based on their intensity and vertical depth? Do these classifications differ in  
80 terms of their spatial distribution and temporal variability? How is the spatial distribution of COLs in the Southern  
Hemisphere related to their vertical depth?

2.3. How do jet streams influence COLs? What Does the influence on deepening mechanisms differ between different  
COL types drive the vertical extension of COLs? Can specific jet stream characteristics be identified as particularly  
conducive to the deepening of COLs?

85 By addressing these key questions, we hope to gain valuable insights into the deepening process and spatial characteristics of  
COLs along with a comprehensive significantly improve our understanding of COLs and their role in atmospheric dynamics  
the underlying mechanisms that govern their vertical extent. The remainder of the paper is organized as follows. Section 2  
outlines the data and methods employed for tracking, estimating vertical depth, and calculating the EKE budget producing  
composites of structure and energetics of COLs. Section 3 presents the results, and finally, Section 4 provides a summary of  
90 the main findings and conclusions.

## 2 Data and ~~Methodology~~ methods

### 2.1 Reanalysis dataset and tracking methodology

This study uses the ERA-Interim reanalysis data (~~hereafter ERAI~~; Dee et al. 2011) obtained from the European Centre for Medium-Range Weather Forecasts (ECMWF) for the period from 1979 to 2014. ~~The ERAI ERA-Interim~~ reanalysis employs a spectral model with a N128 reduced Gaussian grid (~80km) and 60 vertical hybrid levels, produced with a four-dimensional variational data assimilation (4D-Var) system.

Before the tracking, the data are spectrally truncated at 42 wavenumbers (T42), and coefficients corresponding to total wavenumbers less than five are set to zero. This is done to reduce noise and eliminate large-scale background influences, similarly ~~to previous work as done before~~ (Pinheiro et al. 2017; 2021; 2022). The established TRACK algorithm (Hodges 1995, 1996, 1999) is employed to track T42 vorticity minima at various pressure levels (1000, 900, 800, 700, 600, 500, 400 and 300 hPa), using a consistent threshold ( $-1.0 \times 10^{-5} \text{ s}^{-1}$ ) intentionally set relatively low to capture diverse cyclonic systems. The tracking is performed by minimizing a cost-function for track smoothness subject to adaptive constraints on track smoothness and displacement distance. The tracking is the same ~~method-algorithm~~ as used for extratropical and tropical cyclones (e.g., Hodges et al. 2011, 2017), but with some adjustments to the slower ~~moment-movement~~ of COLs, as discussed in Pinheiro et al. (2019). The resulting tracks are filtered based on horizontal wind components (u, v) ~~in~~ at four 5° geodesic ~~5° geodesic~~ offset points from the vorticity center: 0° (u>0), 90° (v<0), 180° (u<0) and 270° (v>0) relative to north. This retains only closed cyclonic centers, as discussed in Pinheiro et al. (2019). The retained tracks are those that either move equatorward and reach latitudes north of 40°S or originate north of 40°S and persist for at least 24 hours.

Spatial statistics of the COLs are computed using the track information and spherical kernel estimators for track density and mean intensity (Hodges 1996). Track density represents COLs per season per unit area ( $5^\circ$  spherical cap  $\cong 10^6 \text{ km}^2$ ), while mean intensity derives from T42 relative vorticity, scaled by -1 for the Southern Hemisphere. ~~Additionally, feature density is calculated using all track points, implying a concentrated density contribution in a small region for slow moving systems due to the higher point density.~~

### 2.2 Approach to ~~determine-estimate~~ the ~~COL~~ vertical depth of COLs

To analyze and quantify COLs, numerous algorithms have emerged, though only a few of them address multi-level cyclone detection and their connections. Existing algorithms establish cyclone position correspondence between levels based on feature point distances, utilizing mean sea level pressure/geopotential or vorticity centers. These methods span from basic search tasks (Lim and Simmonds 2007, Porcù et al. 2007) to more advanced techniques based on optimal solution (Lakkis et al. 2019).

In this study, the track matching algorithm introduced by Hodges et al. (2003) and used to match tracks in different datasets (Bengtsson et al. 2009, Hodges et al. 2011, 2017, Pinheiro et al. 2020) is employed to match tracks between different

pressure levels. The algorithm is used to compare tracks across different pressure levels by defining a mean separation distance ( $d_m$ ), chosen here to be 5 degrees geodesic, and considering overlaps in time ( $\chi$ ) between corresponding points in the tracks. Temporal overlaps between tracks will be determined following a sensitivity analysis, as discussed in Section 3.1.

125 The percentage of points overlapping in time is calculated using the approach described in Hodges et al. (2003), defined as follows:

$$\chi = 100[2n_m/(n_1 + n_2)]$$

where  $n_m$  is the number of points that match in time, and  $n_1$  and  $n_2$  are the number of points in the track corresponding to different pressure levels.

130 ~~Since our focus is on the upper-level forcing driving surface cyclone development and the mechanisms governing this interaction. Assuming the COL development from upper to lower levels (Nieto et al. 2005), our method works top-down, starting at 300 hPa, starting with two levels at a time and progressively extending the matches to adjacent pressure levels.~~ Vorticity tracks ( $\xi_{300}$ ) are matched against  $\xi_{400}$  if mean separation distance is  $\leq 5^\circ$  and temporal overlap exists. Successful matches indicate extending COLs; unmatched  $\xi_{300}$  tracks imply the COL is confined to 300 hPa. An iterative process  
135 continues to lower levels (e.g., 500 hPa, 600 hPa, and so on), stopping at the last match ~~or~~ at 1000 hPa. The deepest successful match determines the COL vertical extent.

~~Complex interactions between COLs and lower-level cyclonic features makes capturing the full range of coupling processes challenging. While ~~o~~Our algorithm, ~~while is~~ simpler than the optimal solution-based ~~one approach~~ in Lakkis et al. (2019), ~~it consistently~~ establishes ~~consistent~~ vertical associations and a sequential stacking process. ~~allowing a track stacking approach. Similar to their method, we start with two levels at a time and progressively extend the matches to adjacent pressure levels, enabling a sequential stacking process. It is important to note that COL deepening can exhibit varied characteristics and evolution across pressure levels, then a top-bottom approach might not capture all coupling types.~~ ~~Consequently~~ However, diverse matching procedures ~~can might lead result to varying in~~ distinct COL evolution outcomes, although prior research has shown similar results between bottom-to-top and top-to-bottom approaches (Lakkis et al. 2019).~~

### 145 **2.3 Energetic diagnosis**

#### **2.3 Compositing analysis of the structure and energetics of COLs**

Employing a system-centered compositing method similar to that of Pinheiro et al. (2022), we investigate the composite structure of COLs and their eddy kinetic energy (EKE) budget. Initially, COLs are identified and categorized into shallow and deep types based on their vertical extent. Shallow COLs are limited to the upper troposphere, extending no lower than  
150 400 hPa, while deep COLs originate at high levels and extend down to 800 hPa or lower. Additionally, we classify COLs as strong (above the 50th percentile) or weak (below the 50th percentile) according to their intensity, based on the 300-hPa vorticity.

155 Atmospheric fields and energetic quantities are sampled on a 25° latitude-longitude rectangular grid, initially defined centered on the equator then rotated to the COL 300hPa vorticity center, with a horizontal resolution of 0.5°. The sampling is performed at each vertical level from 1000 hPa to 100 hPa, taking the 300-hPa track point as the reference. We present vertical composites for west-east cross-sections centered on the vorticity center. These composites are produced for various time intervals relative to the peak intensity of COLs, but only for times within ± 48 hours of the peak intensity are shown. Extending the compositing window beyond this timeframe often introduces noise due to variations in COL lifetimes.

160 Analyzing the EKE budget is a valuable approach for studying the development of COLs (Gan and Piva 2013, 2016, Pinheiro et al. 2022). In the present study, we employ the EKE budget to Using the Orlanski and Katzfey (1991) method, we investigate the energy dynamics associated with the COL deepening of COLs through the EKE budget. This is done by utilizing the methodology developed by Orlanski and Katzfey (1991), which incorporates approach considers essential mechanisms including such as baroclinic and barotropic conversions as well as and ageostrophic flux convergence, commonly known as (downstream development). In this study, the focus is on baroclinic conversion and ageostrophic flux convergence, the two primary EKE budget mechanisms in COLs (Gan and Piva 2016, Ndarana et al. 2021, Pinheiro et al. 2022). The components of the EKE budget are computed as follows:

$$165 \frac{\partial(K^t)}{\partial t} = -\langle \nabla \cdot \bar{V}_a^t \phi^t \rangle - \langle \omega^t \alpha^t \rangle - \left[ \bar{V}^t \cdot (\bar{V}_3^t \cdot \nabla_3) \bar{V}^t + \bar{V}^t \cdot (\overline{\bar{V}_3^t \cdot \nabla_3}) \bar{V}^t \right] + ADD + RES \quad (1)$$

170 Here,  $K$  is the kinetic energy,  $\bar{V}$  the horizontal wind,  $\phi$  the geopotential,  $\omega$  the vertical velocity, and  $\alpha$  the specific volume. Overbars represent the time mean calculated for each month and year, primes the eddy part, subscripts  $a$  the ageostrophic component, and superscripts 3 the three dimensional vector. The symbol  $\langle \rangle$  denotes volume integrals computed from the bottom (taken as the surface pressure) to the top (referred to the 100 hPa level).

175 In Equation 1, the 1st term on the right hand side is the ageostrophic flux convergence, the 2nd term is the baroclinic conversion, the 3rd and 4th terms are the barotropic conversion, the 5th term ( $ADD$ ) are additional terms which have small contribution for the EKE budget, such as the vertical advection of energy through the upper and lower boundaries. The budget residual (6th term,  $RES$ ) represents accounts for processes or factors not fully accounted captured for in by the EKE budget equation calculation. These include, including friction, diabatic effects, and discretization errors such as interpolation and finite differences. It could also arise from analysis increments due to data assimilation, affecting the energetics. Errors could also arise from how Diabatic heating estimates from processes are represented in reanalysis products, reliant on microphysical processes, are significantly influenced by assimilation moist process parameterization (Pinheiro et al. 2022).

180 Time-mean quantities are calculated for each month averaged over 28–31 days for the 6-hourly data, separately for each individual month and year. The residual is computed by taking the difference between the observed/diagnosed EKE change (left hand side, LHS) and the sum of known contributing EKE budget terms (right hand side, RHS).

The energetics are computed by referencing the terms of Equation 1 to the tracks in a radial grid of 15°-geodesic centered on the COL center, following the approach previously used in Pinheiro et al. (2022). The computation is performed in two ways: separately at each pressure level and integrated from 1000 hPa (or surface) to 100 hPa. Our analysis in this paper focuses on the two primary mechanisms of the EKE budget in COLs which are baroclinic conversion and ageostrophic flux convergence. Analyses are performed for each season, but only the mean fields are presented in the main text for simplicity and convenience.

## 2.4 Link with jet streams

The connection between COL extent and jet streams is also explored. Following Bals-Elshol et al. (2001), the characteristics of the polar front and subtropical jets are defined by averaging the 300-hPa zonal mean zonal wind at 50°S-65°S and 25°S-35°S, respectively. Despite the high variability in wind speed, jet streams exhibit relatively small seasonal variations in the Southern Hemisphere (Simmons and Jones 1998), allowing a reasonable estimation using upper-tropospheric zonal mean winds within a fixed latitudinal band. Pearson correlation coefficients are employed to verify the relationship between jet strengths and COLs, with significance exceeding 95% and 99%.

## 3 Results and discussion

### 3.1 Sensitivity of track matching algorithm for the estimation of COL depth

To assess the sensitivity of the track matching algorithm regarding the computation of in determining COL depth, we investigate the influence of the mean separation distance ( $d_m$ ) and temporal overlap ( $\chi$ ) between tracks at different pressure levels. Specifically, we systematically varied vary the value of  $\chi$  from 1% to 100% while keeping the threshold  $d_m$  fixed at 5° geodesic. This choice is based on observations that the estimation of the depth estimation is more sensitive to changes in  $\chi$  than to  $d_m$ . It is worth noting that making Setting  $d_m$  to a too-large value leads to a significant rise in the number of matches; however, this can will introduce false matches involving unrelated cyclonic systems, particularly when using vorticity, which emphasizes small spatial scale features. Therefore, we set the parameter  $d_m$  to 5 degrees geodesic, a value which is suitable for this study, considering that the typical small vertical tilt of COLs is typically much smaller than this threshold (refer to Fig. 9 in Pinheiro et al. 2021).

A sensitivity analysis is designed by varying the parameter varied  $\chi$  across a range of values. Setting  $\chi$  to 1% requires that the mean separation distance a minimum 1% time overlap between tracks at different pressure levels is satisfied with an overlap in time of at least 1% for the corresponding track points. Based on the results presented in Table A.1 of the in the Appendix, it was found that shows that 20.3% of the  $\xi_{300}$  COLs extend all the way to the surface during in at least one time step, indicating the presence of interconnected cyclonic features across all levels from 300 hPa to 1000 hPa. The number of systems reaching the surface remains relatively consistent for  $\chi$  values ranging from 1% to 25%, corresponding to percentages ranging from at 20.3% to 19.5% of all COLs. However, there is a matches significantly decrease in the number of matches when  $\chi$  exceeds 50%, likely due to COLs only associating briefly with lower-level features. This observation

215 suggests that the coupling between upper and lower levels may occur more frequently during the mature to decay stages of  
the COL life cycle, influencing the number of matches. When  $\chi$  is set to 75%, indicating a large overlap threshold, less  
than 10% of systems are identified as deep COLs, suggesting an underestimation due to association with short-lived lower-  
level features. These findings indicate that using a high  $\chi$  value restricts the number of matches, resulting in an  
underestimation of labeled deep systems. Although determining the optimal threshold for establishing correspondence  
220 between upper and lower level low pressure systems is challenging, employing a small  $\chi$  value threshold  
increases the chance of appears suitable for this task as it ensures capturing at least one time step during the life cycle of a  
well defined stacked cyclonic system. To address this, the analysis of COL depth in this study adopts  $\chi=1\%$  and  $d_m=5$ .  
This implies that the mean separation distance between tracks at adjacent pressure levels is less than 5 degrees, and there is  
overlap in time for at least one track point. This criterion guarantees that COLs are guaranteeing vertically aligned or tilted  
225 COLs across adjacent levels using  $\chi=1\%$  and  $d_m=5^\circ$  at the designated pressure level, as demonstrated in Pinheiro et al.  
(2021).

Using geopotential data instead of relative vorticity to estimate the vertical COL depth of COLs offers is an alternative  
approach. However, some care is required in selecting an appropriate threshold as geopotential magnitude generally  
increases with height in baroclinic systems. Previous studies (Porcù et al. 2007, Barnes et al. 2021) used varying geopotential  
230 thresholds for each pressure level to obtain vertical depth, which requires, requiring different subjective thresholds at each  
level. In contrast, vorticity-based identification does not require adjusting the threshold according to pressure level vertical  
adjustments, as vorticity measures the atmospheric flow's rotation. Moreover, weaker vorticity COLs are less likely to be  
identified in the a geopotential field-based tracking method. (Pinheiro et al. 2019).

### 3.2 Regional differences in COL depths

235 Based on the algorithm outlined in Section 2.2, three categories of COLs based on their vertical extents are proposed:  
shallow, medium, and deep COLs. Shallow COLs (Figure 3a) are defined as low pressure systems primarily confined to the  
upper troposphere, not extending lower than 400 hPa. Medium COLs (Figure 3b) are defined as originating at high levels  
and extending down to between 500 hPa, and 700 hPa. Deep COLs (Figure 3c) are defined as developing at 300 hPa and  
extending down to 800 hPa or lower. Although deep COLs can exhibit tilted or stacked structures, this analysis does not  
240 consider the vertical tilt. A discussion on the vertical tilt of COLs has been addressed by Pinheiro et al. (2021).

### 3.2 Relationship between intensity and vertical depth of COLs

Classifying COLs by grouping similar systems is crucial for uncovering the key factors influencing their diverse types,  
allowing a deeper understanding of their dynamics and providing a framework for evaluating climate impacts. This section  
explores the contrasting characteristics among four COL categories: shallow, deep, weak, and strong COLs (Figure 1). These  
245 categories are defined based on intensity and vertical extent, as detailed in Section 2.2. While intermediate-level COLs exist,

this study focuses on the contrasting features of their vertical extent. This analysis does not focus on vertical tilt, which is comprehensively addressed in Pinheiro et al. (2021).

250

Figure 1 shows the annual track density of COLs in the four categories described above. Deep and strong systems exhibit similar distribution patterns, both primarily concentrated in Australia and the southwestern Pacific, with a secondary maximum in the southeast Pacific off the west coast of South America. These two groups exhibit similar intensity patterns, with maxima (blue dots) located in Australia and upstream of the main continents, as previously demonstrated (Barnes et al. 2021, Pinheiro et al. 2021, 2022). Shallow and weak COLs also share similarities; they are less intense and more dispersed than the deep and strong systems. These systems are predominantly found in the South Atlantic, southeast Africa (Madagascar), and the South Indian Ocean, and they are more frequently found equatorward than their deep and strong counterparts, a notable feature over the central-eastern Pacific Ocean.

255

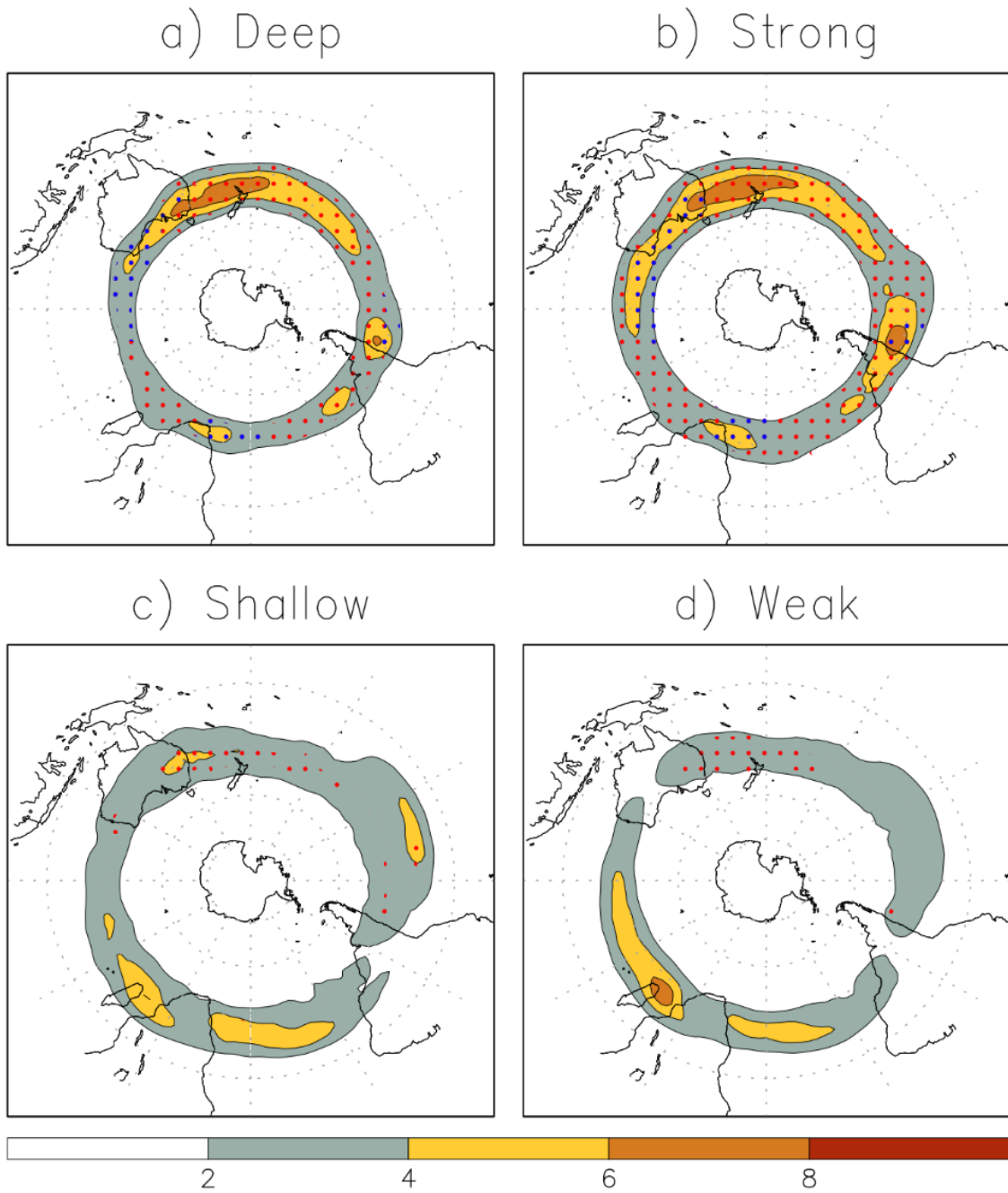


**Figure 13:** Track density (shaded) and mean intensity (contours and dots) for (a) shallow-deep, (b) medium-strong, and (c) shallow, and (d) weak deep-COLs in the Southern Hemisphere. Track density is measured in number per season per unit area, where the unit area is equivalent to a  $5^\circ$  spherical cap ( $\approx 10^6 \text{ km}^2$ ). Mean intensities less than  $-8 \times 10^{-5} \text{ s}^{-1}$  ( $-12 \times 10^{-5} \text{ s}^{-1}$ ) are represented in red (blue) dots. Unit is the same as in Figure 1.

Figure 3 demonstrates substantial regional variations in the distribution of COLs based on their vertical extents. There are regions that exhibit a high concentration of deep COLs, as in the eastern Australia, New Zealand, and western Pacific. The split jet structure during austral winter may be one reason why COLs are deeper in the Australian region, as this causes vorticity advection and deepens the trough-ridge system (Ndarana et al. 2020). Additionally, the southwestern Atlantic Ocean, especially that neighboring South America, is another preferred location for deep COLs. In contrast, the COLs found in the southeast Africa and South Indian Ocean regions predominantly consist of shallow and medium depth systems.

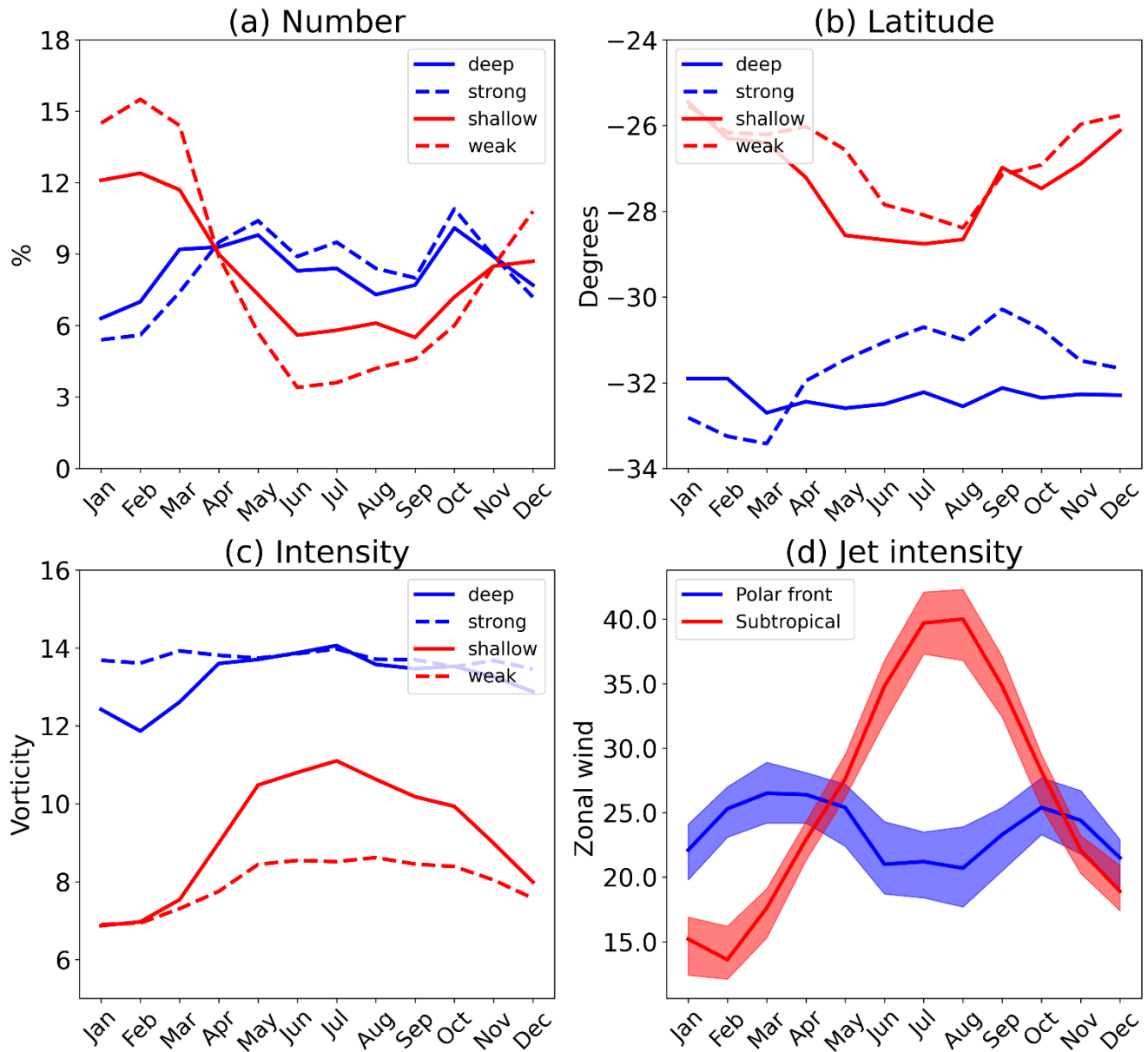
We found that the vertical extent of COLs varies with latitude, with shallow COLs occurring at all latitudes, while deep COLs are more prevalent at higher latitudes and less frequent north of 30°S. One interesting exception to this pattern is found in the southeastern Pacific, where deep, strong COLs can be observed at more northern latitudes than in other regions. This phenomenon aligns with the high mean intensity of COLs near the central coast of Chile, as shown in Figure 1e and previously discussed in Vuille and Ammann (1997).

Figure 2 shows the seasonal variations in the average monthly number, intensity and latitude of COLs for each of the four distinct categories. A clear correspondence in seasonality is evident between deep and strong COLs, as well as between shallow and weak types. Deep and strong COLs exhibit similar intensities (Fig. 2c), though the deepest systems display a more pronounced seasonal cycle in intensity compared to the strongest ones. Deep and strong COLs are more prevalent at 31-33°S (Fig. 2b) from autumn to spring, with two peaks in May and October (Fig. 2a). These peaks appear to be associated with a semiannual oscillation in the polar front jet, albeit with two-month delay from the first peak (Fig. 2d). The half-yearly cycle in the eddy-driven jet is attributed to a response of meridional temperature and pressure gradients between middle and high latitudes which peaks during equinoctial seasons (Van Loon 1967). Our findings align with previous studies and demonstrate a similar cycle to that observed for mid-latitude COLs and Rossby wave breaking events on the 330 K isentropic surface (Ndarana and Waugh 2010, Favre et al. 2012).

In summer, shallow and weak COLs exhibit notably higher frequencies compared to the fewer occurrences observed in winter months. This seasonal pattern appears to be closely linked to the fluctuations in subtropical jet intensity, which experiences a decline (increase) in summer (winter). The increased (reduced) frequency of COLs appears to correspond with the weakened (intensified) subtropical jet strength in summer (winter). This association likely arises because shallow and weak COLs tend to occur more equatorward, roughly coinciding with the subtropical jet position (see Fig. 3). This aligns with the idea that COLs are primarily found over regions of weakened westerly winds (Nieto et al. 1998), and this hypothesis is supported by a robust negative correlation of -0.95 (-0.97) significant at 95% between shallow (weak) COLs and subtropical jet intensity.

Overall, there exists a discernible relationship between upper-tropospheric intensity of COLs and their vertical depth, establishing both classifications as pertinent parameters for assessing the vertical structure of these phenomena. The association of deeper COLs with stronger cyclonic vorticity can be attributed to geostrophic balance and the vertical

coupling of atmospheric motions. Enhanced upper-tropospheric circulations induce increased vertical motions and static stability anomalies, resulting in the formation of deeper vertical structures. To maintain consistency and simplicity in our analysis, our subsequent investigations will solely concentrate on the classification based on COL depth.



**Figure 2:** Zonal monthly mean characteristics of COLs categorized by deep, strong, shallow and weak for: a) number, b) latitude reached at the time of maximum intensity, and c) maximum intensity (300-hPa vorticity). d) Intensity of subtropical latitude reached at the time of maximum intensity.

and polar front jets as represented by the climatological 300-hPa zonal mean zonal wind at 25°S-35°S and 50°S-65°S, respectively.

### **3.3 Seasonal variations in Jet-COL interactions**

The interplay between COLs, jet streams, and Rossby wave breaking has been documented in previous studies (Ndarana and Waugh 2010, Barnes et al. 2021). To unravel this relationship further and elucidate how jets influence COL deepening, we present seasonal mean maps of upper-level zonal winds and track density for deep and shallow COLs, as illustrated in Figure 3. A distinct polar front jet, often referenced as the mid-latitude jet in literature, is apparent from the South Atlantic to the South Pacific oceans throughout the year, exhibiting a poleward spiraling pattern. In the Australia-New Zealand sector, the well-known split jet flow becomes more pronounced during the cool season due to a stronger subtropical jet (Fig. 3c). This pattern results in weak westerlies between the jets, inducing anticyclonic vorticity on the equatorward side of the subtropical jet and cyclonic vorticity poleward (refer to Fig. S2 in Suppl. Material).

As previously discussed, deep COLs tend to be situated at more poleward latitudes, typically near the equatorward exit region of the polar front jet. This is particularly noticeable around Australia throughout the year, albeit with some seasonal and spatial variations. During winter, COLs are less frequent but more intense than other seasons (see Fig. 2), likely due to an intense subtropical jet, which generates cyclonic vorticity anomalies over its poleward side. Conversely, the subtropical jet is weak or absent in summer, leading to a higher occurrence of shallow, weak COLs closer to the equator and over the oceans. Interestingly, deep COLs peak in autumn and spring, coinciding with a strengthened polar front jet which reaches a comparable magnitude to the subtropical jet. Additionally, during the transitional seasons, a secondary maximum in deep COLs is observed near the west coast of South America, particularly in spring when the maximum density occurs with reduced zonal flow at the end of the polar front jet on the poleward side of the subtropical jet.

Our findings suggest that the position and strength of the jet streams influence the vertical structure of COL. This is supported by earlier observations of a stronger polar front jet leading to a more pronounced dipole pattern with enhanced cyclonic and anticyclonic vorticity anomalies (Bals-Elshol et al. 2001).

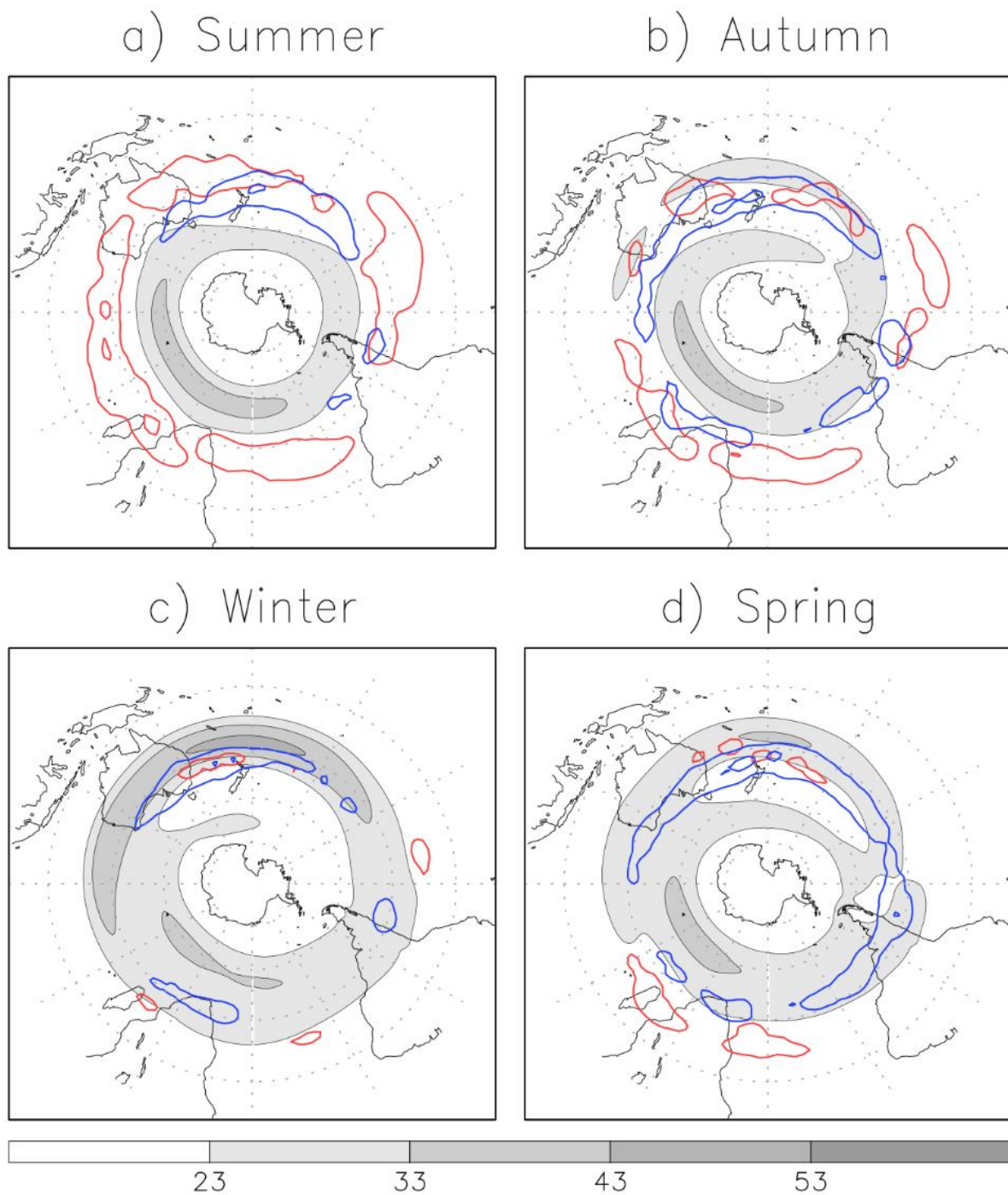


**Figure 3:** Zonal mean wind (shaded) and track density for deep COLs (blue contour) and shallow COLs (red contour) in the Southern Hemisphere for a) Summer (DJF), b) Autumn (MAM), c) Winter (JJA) and d) Spring (SON). Unit is as in Fig. 1

325 for track density, and  $\text{m.s}^{-1}$  for zonal wind. Track densities are plotted for interval contours of 4 units. All fields are represented at the 300-hPa level.

### **3.4 Distinct effects of polar front and subtropical jets on COL depths**

330 To further investigate the influence of jets on COLs, scatter plots are employed to visualize the relationship between COLs and different jet intensities, as given in Figure 4. Deep COLs exhibit a moderate positive correlation with the polar front jet intensity ( $r = 0.47$  at 99% confidence level), indicating that an intensifying jet promotes an increase in deep COLs. This correlation accounts for approximately 22% of the variability in deep COLs. Shallow COLs also show a positive correlation with the polar front jet intensity, but it is weaker than that for deep COLs ( $r = 0.25$ ,  $p < 0.01$ ), explaining only 6% of their variability.

335 Considering the subtropical jet (Fig. 4b), there seems to be almost no significant relationship to the occurrence of deep COLs, with an insignificant correlation coefficient and a trend line that suggests no meaningful association. However, for shallow COLs, there exists a significant negative correlation of 0.75 (99% confidence level), indicating that intensified subtropical jet is related to reduced shallow COLs. Approximately 56% of the variability in shallow COLs can be attributed to changes in subtropical jet intensity, aligning with their seasonal variations (as referred to Fig. 2). While the relationship between COL intensity and jet intensity has been examined in this study, no significant correlations were found. This

340 suggests that jets primarily influence the frequency rather than the intensity of COLs.

These differential effects are likely due to the distinct roles that polar front and subtropical jets play in the large-scale atmospheric circulation. The polar front jet, primarily occurring at mid- and high-latitudes, is an eddy-driven jet associated with strong temperature gradients and baroclinicity. In contrast, the subtropical jet, situated around  $25^{\circ}$ – $30^{\circ}$ S, arises from the momentum flux of the meridional circulation at the Hadley cell edge. While the subtropical jet clearly influences shallow

345 COLs that occur more often equatorward, the polar front jet appears to act as a precondition for deepening COLs at more poleward latitudes.

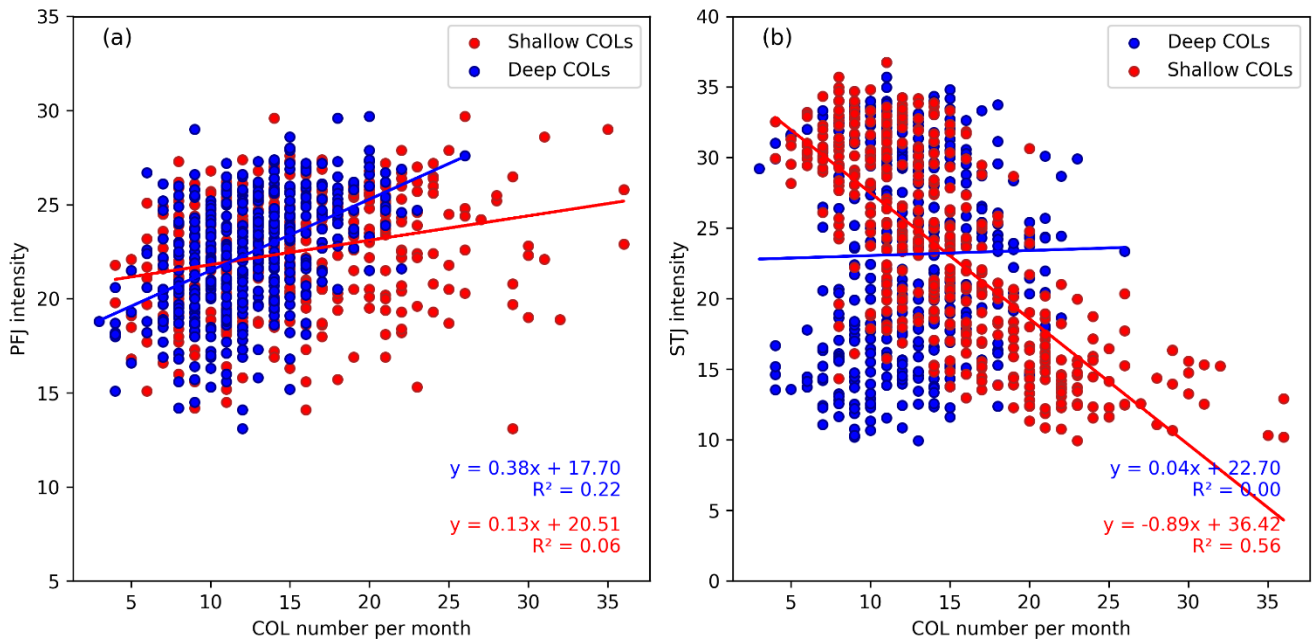


**Figure 4:** Scatter plots indicating the relationships between monthly mean COL number and jet intensity for (a) polar front jet and (b) subtropical jet. Deep and shallow COLs are depicted by blue and red colors, respectively. Unit is in m/s for jet intensity.

### 3.3 Spatial variability of shallow, medium and deep COLs

Studying the regional variations in the vertical extent of COLs is important for understanding the associated weather patterns, enhancing forecasting accuracy, and assessing the potential impacts on diverse regions. The recent study by Barnes et al. (2021) analyzed COL extent in South America, South Africa and the Australia New Zealand region. Their findings revealed that deep COLs appear to be more prevalent in Australia and New Zealand, while relatively shallower COLs are observed in the southern African region. Expanding on their study, we conduct an analysis of eight distinct genesis maxima regions in the Southern Hemisphere (Figure 1a). This approach allows for a more detailed examination of regional differences in the vertical extent of COLs. By using the tracks identified by Pinheiro et al. (2022 in Section 2.2, we determine the lowest pressure level reached by the upper level COL throughout its entire life cycle.

Figure 2 illustrates the variations in COL depth across pressure levels and regions. We adopt the conceptual evolution of COLs that develop at upper levels and extend downwards to the surface (Nieto et al. 2005). Our results indicate that the vertical extent of COLs is relatively consistent in the upper troposphere but exhibits more significant differences below 500 hPa. Deep COLs are more frequent in regions E, F (southeast Australia), and H (southwest Atlantic Ocean), with approximately 30% of total COLs extending all the way to the surface. Recent research by Pinheiro et al. (2022) has

365 highlighted the significance of baroclinic conversion as the main EKE contributor for the COLs in regions E, F and H, suggesting a potential mechanism for their deepening.

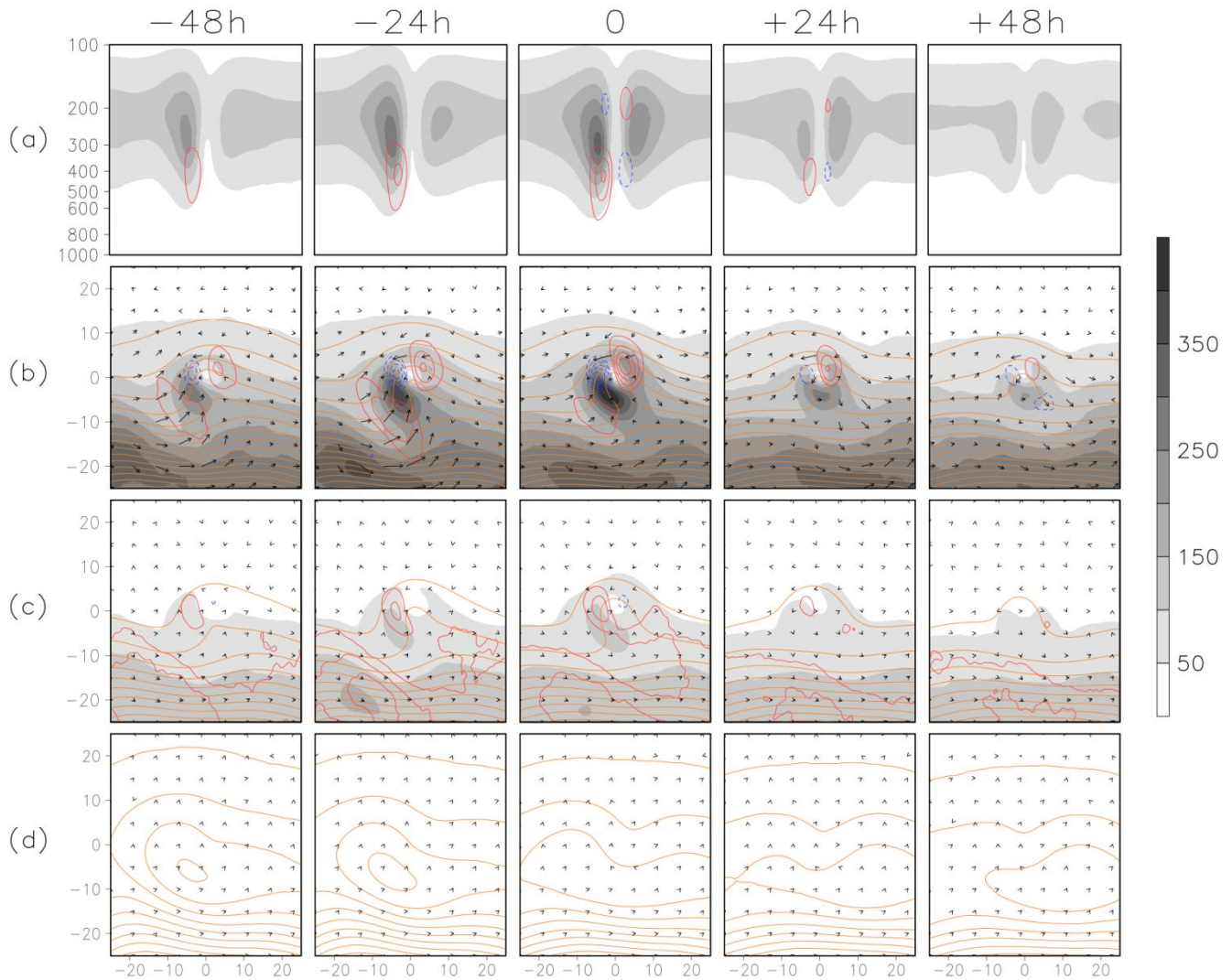
Interestingly, there are regions where COLs extend to lower levels as much as the deepest observed systems do, but the extents reduce dramatically at levels below 800 hPa. This is particularly the case for the region G COLs (South East Pacific). A similar sharp decrease in the number that fully extend to the lowest level occurs for the regions A and C COLs (South East Atlantic and South East Indian Ocean).

370 According to Pinheiro et al. (2022), these COLs share common attributes: COLs that originate in regions A, C and G are situated upstream of the major continents and are dominated by upper level ageostrophic fluxes, possibly associated with stationary Rossby waves. Considering the entire Southern Hemisphere, our analysis demonstrates a relatively homogeneous distribution of COL extents between 300 and 600 hPa. However, extents between 700 and 900 hPa are less common, aligning with the findings of Barnes et al. (2021). In contrast to their previously reported 51.7% fully extended COLs, our analysis suggests that only 20.3% of COLs extend all the way to the surface. These differences may arise from methodological variations, as previous studies relied on the geopotential (Porcù et al. 2007, Barnes et al. 2021), which is less sensitive to identifying weaker systems (Pinheiro et al. 2019). As vorticity is better at detecting weaker systems than geopotential, resulting in differences in the total identified systems, vorticity is expected to identify fewer deep COLs as a proportion of all systems. Moreover, earlier studies likely included numerous higher latitude vortices, which predominantly exhibit a deep vertical structure. Barnes et al. (2021) highlight that excluding more poleward latitude COLs minimizes these discrepancies.

### 3.4.3.5 Shallow COLs vs deep COLs: contrasting from the energetics point of view

When it comes to unraveling the intricate mechanisms behind the deepening of COLs, understanding the role of specific mechanisms in determining their vertical extent can be aided by examining their energetics. Early studies have investigated the dynamical mechanisms of COLs by examining their vertically integrated energy budgets (Gan and Piva 2013, 2016, Ndarana et al. 2020, Pinheiro et al. 2022). In this study, we adopt a similar approach but direct our attention towards the two primary contributing mechanisms of the EKE budget: baroclinic conversion and ageostrophic flux convergence. We compare deep and shallow COLs and investigate the possible implications of energetics for their deepening.

390 Figures 4-5 and 5-6 show the temporal evolution of composite shallow and deep COLs, respectively, for horizontal and vertical fields. The four stages described in the conceptual model of Nieto et al. (2005) and shown in Pinheiro et al. (2021) are seen to be reproduced for shallow and deep COLs, involving the following stages: upper-level trough (-48h), tear-off (-24h), cut-off (0), and decay or dissipation (+24 and +48h). Time is referenced to the time of maximum intensity in the 300 hPa vorticity.



395

400

**Figure 4-5** Temporal evolution of shallow COLs in the Southern Hemisphere relative to the time and space of maximum intensity in  $\xi_{300}$ . The panels depict: (a) vertical cross-sections of total EKE (shaded) with baroclinic conversion (contour); (b) vertically integrated ageostrophic flux convergence (contour) with EKE (shaded), geopotential height (orange line) and ageostrophic fluxes (vectors) at 300 hPa; (c) vertically integrated baroclinic conversion (red contour) with EKE (shaded), geopotential height (orange line) and ageostrophic fluxes (vectors) at 500 hPa; and (d) EKE, geopotential height (orange line) and ageostrophic fluxes (vectors) at 1000 hPa. Contours represent  $0.003 \times 10^{10}$  Joule. $s^{-1}$  for integrated quantities, 50 gpm for geopotential height at 300 and 500 hPa, and 20 gpm for geopotential height at 1000 hPa, while total EKE is indicated by  $10^9$  Joule.

405 ~~During~~In the upper-level trough and tear-off stages of shallow COLs ( $T = -48\text{h}$  and  $T = -24\text{h}$  in ~~Figure 4~~Fig. 5), the mid-latitude ~~a poleward jet~~ located upstream of the ridge axis, i.e., west of the COL, acts as the primary energy source of energy for the COLs. Concurrently, ageostrophic fluxes transport EKE northeastward from the poleward jet stream to the rear side of the COLs, forming an westward energy center downstream of the ridge axis, referred to as the western energy center, ~~as observed by Gan and Piva (2013).~~ As the ~~system intensifies,~~ this trough-ridge system deepens in an anticyclonic orientation, the western energy center expands due to the convergence of ageostrophic fluxes and positive baroclinic conversion that  
410 arises downstream of the ridge axis occurring to the west of the COL, driven by descending cold air (not shown) ~~(refer to the supporting information of Pinheiro et al. 2021).~~ The eastward propagation of the poleward jet and its increasing zonal flow give rises to anticyclonic barotropic shear flow and subsequent potential vorticity overturning, as documented in prior studies (Ndarana et al. 2021, Pinheiro et al. 2022). The COL decay occurs when the poleward jet shifts to the east, ceasing to provide energy to the system.

415 ~~These characteristics resemble those observed in a previous study of intense Southern Hemisphere COLs (Pinheiro et al. 2022).~~ However, it is worth noting that in the case of the stronger COLs, the baroclinic processes and ageostrophic fluxes are much more intense. ~~During the decay stage, baroclinic conversion and ageostrophic fluxes weaken, contributing to the gradual dissipation of the COL.~~

420 Differences in the structure and lifecycle of shallow and deep COLs are observed. While shallow systems exhibit a gradual weakening and anticyclonic circulation at the surface, deep COLs display a multi-level interconnected vortex structure, as illustrated in Figure 6. During their ~~The development phase, described above occurs similarly in deep COLs systems,~~ as depicted in Figure 5. However, the energy growth in deep COLs occurs more vigorously ~~due to the presence of~~ exhibit stronger ageostrophic fluxes along the ridge axis, on the rear side of the COL. Moreover, there is ~~enhanced~~ and larger baroclinic conversion on the upstream poleward jet compared to shallow systems upstream of the COL which is. This  
425 enhanced activity is accompanied by momentum transfer from the upstream poleward jet into the COL. This robust characteristic, linked to the stationary nature of Rossby waves, distinguishes deep COLs from typical mid-latitude disturbances (Chang 2000, Danielson et al. 2006).

430 A distinct aspect of deep COLs arises during the cut-off stage ( $T = 0$  onward), when enhanced vertical motions drive increased baroclinic conversion towards the east and near the surface. The interaction between upper- and lower-tropospheric eddies, as in mid-latitudes baroclinic waves (Hoskins and Karoly 1981, Trenberth 1991, Nakamura 1992), suggests an eddy feedback mechanism between the eddy-driven jet and lower-level thermal forcing (Kushner et al. 2001, Deser et al. 2004, Lu et al. 2014). This feedback likely arises due to thermal wind adjustment (Ring and Plumb 2007, Nie et al. 2016). Additionally, downward eddy momentum activity fluxes also likely contribute to vertical energy propagation, as observed in earlier studies (Trenberth 1991, Rivière et al. 2015).

435 ~~associated with a more intense mid-latitude jet than observed in shallow systems.~~

During the decay stage of deep COLs, ageostrophic fluxes and eddy feedback mechanisms facilitate the downstream export of EKE, maintaining and shifting the jet eastward (refer to Fig. 6 at  $T = +48$ ). The stronger baroclinic processes and

440 ageostrophic fluxes observed in deep systems ~~are likely responsible for explain their~~ longer lifetimes ~~observed in deep COLs~~ (4.7 days) compared to shallow COLs (3.3 days). ~~These factors contribute due~~ to a greater interaction between ~~the~~ mechanisms operating at ~~different various~~ levels within ~~deep COL these~~ systems.

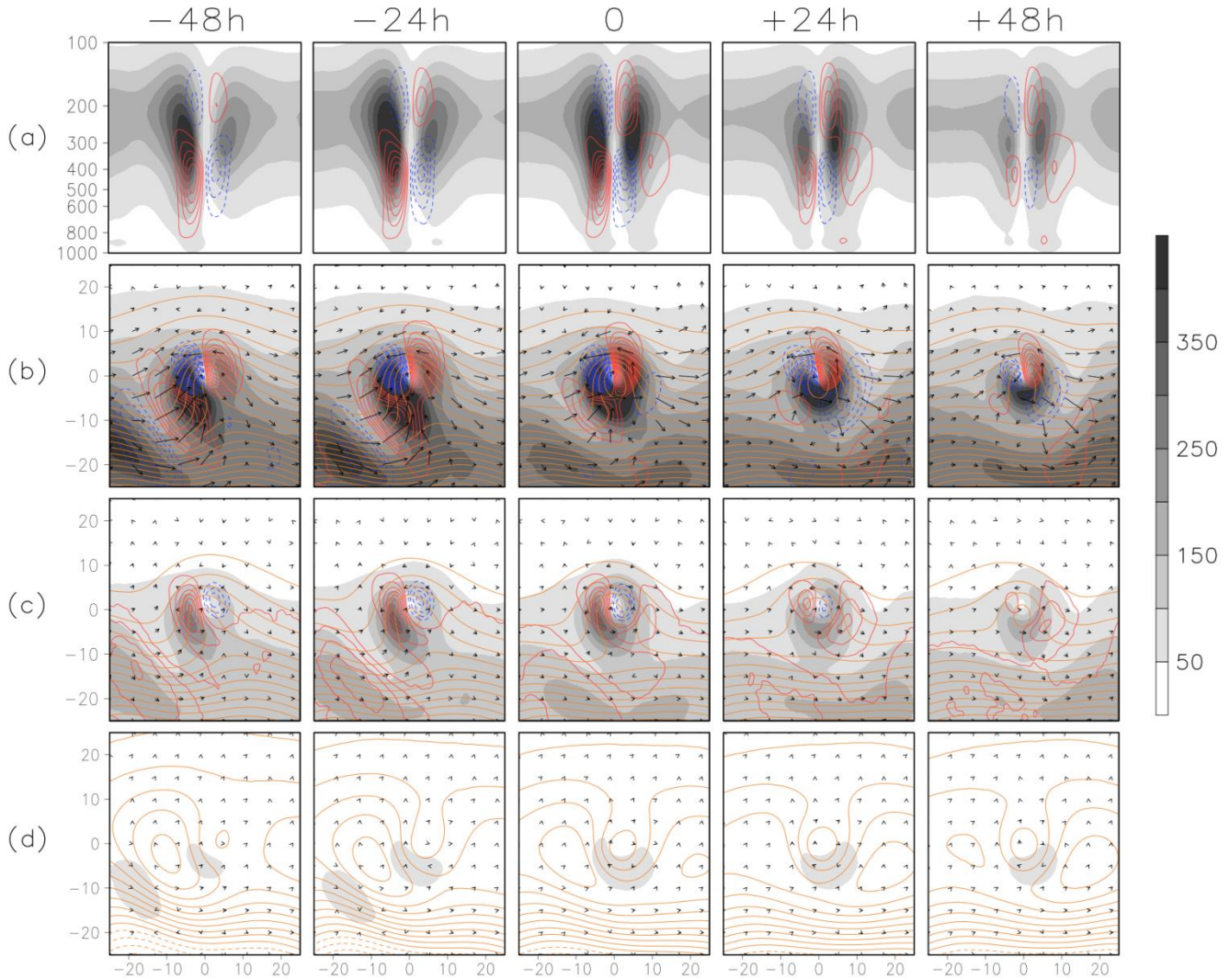


**Figure 56:** Same as Figure 45 but for deep COLs in the Southern Hemisphere. Dashed lines at the bottom indicate negative geopotential height at 1000 hPa.

445 While shallow COLs gradually weaken toward the surface, exhibiting an anticyclonic circulation pattern (see Figure 4d), deep COLs show a distinct multi-level interconnected vortex structure. This notable distinction becomes evident from the cut off to decay stages, particularly when significant positive baroclinic conversion is observed to the east of the deep systems. This is consistent with the findings on strong COLs shown in Pinheiro et al. (2022) and can be attributed to the

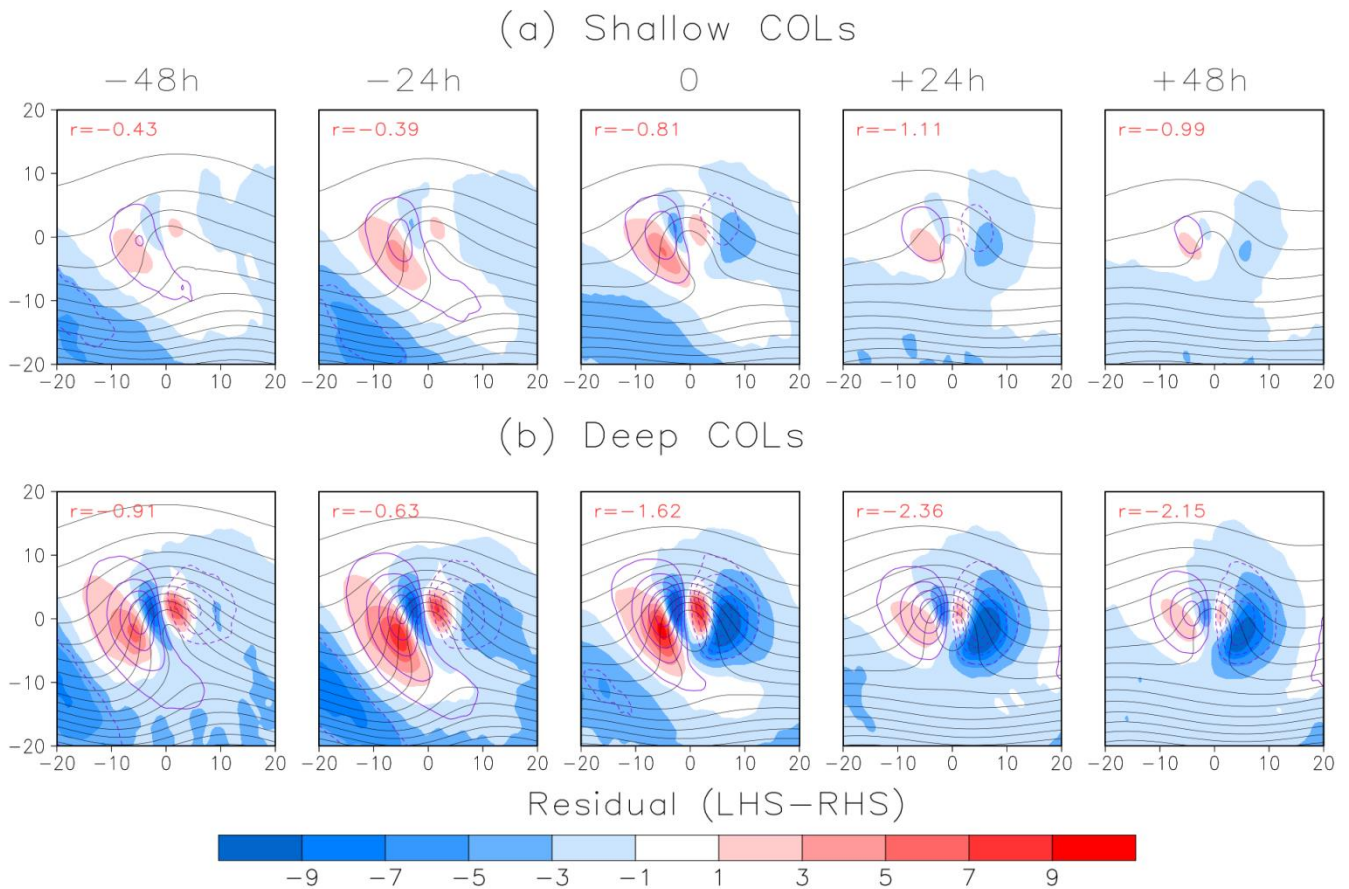
~~combined effect of warm ascent air (thermally direct circulation) and mid-tropospheric diabatic heating. Strong upward vertical motion contributes to the increase in EKE, facilitating the coupling between upper and lower level depressions. Additionally, diabatic heating generates eddy available potential energy which is converted to EKE through baroclinic conversion, as described in Orlanski and Katzfey (1991). This mechanism represents a fundamental forcing for the development of COLs (Cavallo and Hakim 2010). A more detailed discussion on this topic will be provided in the next section.~~

A key feature of our approach lies in its consideration of pre-existing low-level cyclones linked to COLs. This is achieved by using a relatively short temporal threshold for matching, which significantly expands our ability to detect a wide range of multi-level stacked lifecycles. While the results exhibit some sensitivity to the chosen method, they remain remarkably consistent with previous observations of rapid vertical evolution of potential vorticity cut-offs, which typically reach their maximum extent roughly one day after genesis (Portmann et al. 2021). Furthermore, the observed characteristics of deep COLs closely align with patterns identified in Catto (2018) for Cluster 3 and Sinclair and Revell (2000) for Class T in the Australia and New Zealand region, with a cyclone originating directly beneath a deep upper-level trough or a cut-off potential vorticity streamer.

### **3.5 Impacts of diabatic processes on residual energy and its influence in the deepening of COLs**

Numerous studies have demonstrated the influential role of diabatic processes, such as radiation, latent heating and planetary boundary layer processes, in the development of synoptic-scale systems (Davis and Emanuel 1991, Stoelinga, 1996). As pointed out above and discussed in some detail by Pinheiro et al. (2022), inaccuracies arising from the misrepresentation of diabatic heating in reanalyses can introduce uncertainties into the energetic framework. Therefore, investigating the influences of diabatic processes on residual energy can enhance our understanding of their impact on the deepening mechanisms of COLs.

Figure ~~6-7~~ shows the spatial and temporal distribution of residual energy in composites of shallow and deep COLs. The patterns of residual energy exhibit similarities in shallow and deep COLs, with significantly higher magnitudes observed in deep systems. Negative residual energy dominates throughout the lifecycle of both shallow and deep COLs, as indicated by the red values in Figure ~~67~~, representing the residual integrated volume within a 15-degree radial distance centered on the vortex center.



475 **Figure 67:** Temporal evolution of the residual energy in Joule (shaded) scale by  $10^9$ , geopotential height (black contour) at 300 hPa for contour intervals 50 gpm, and vertical velocity (purple contour) for contour intervals  $0.05 \text{ Pa}\cdot\text{s}^{-1}$ , where solid (dashed) contours indicate positive (negative) values. Red values represent the residual energy vertically averaged within a 15-degree spherical cap region centered on the COL location.

480 While negative residual energy prevails, it is worth noting that positive values emerge west of the COLs during the upper-level trough and tear-off stages. Conversely, negative residual energy is observed to the east of the COLs during the cut-off and decay stages. This contrasting pattern is particularly pronounced in deep COLs, consistent with previous findings on strong COLs (see Figure 4 of Pinheiro et al. 2022).

485 The residual energy suggests the existence of development mechanisms that are either not considered in our approach or inadequately represented in the reanalysis data. A common issue lies in accurately representing diabatic processes, such as radiative cooling and latent heating, which pose challenges for reanalysis. A significant negative residual, particularly pronounced in deep COLs, is observed east of COLs where enhanced ascent and convection can introduce additional energy

sources and unresolved phenomena contributing to the residual. In contrast, positive residual prevails along the western COL edge, possibly influenced by sinking air that promotes radiative cooling.

490 Uncertainties in measurement techniques, including inhomogeneous observations, analysis increment, and model parameterizations, are especially important in regions of intense convection. Although diabatic heating does not directly influence the EKE budget as it is not included in the energetic framework, errors in the reanalysis due to the misrepresentation of these processes (see <https://confluence.ecmwf.int/display/FUG/Section+4.2+Analysis+Increments>) can lead to inconsistencies in the energetic analysis, as discussed by Pinheiro et al. (2022). Our results suggest that COLs that are more strongly dependent on diabatic processes are less well represented by reanalysis data.

#### 495 **4 Discussion and conclusions**

500 This study has introduced a track matching algorithm applied to ERA-Interim reanalysis for accurate estimation of COL depth. Our findings highlight that the accuracy of COL depth estimation is primarily influenced by the temporal overlap ( $\gamma$ ) between tracks at different pressure levels. We found that employing  $\gamma = 1\%$  with a mean separation distance of  $5^\circ$  geodesic provides a feasible approach for capturing COLs during specific lifecycle stages. Notably, our method reveals a lower proportion of deep COLs compared to previous studies (Porcù et al. 2007, Barnes et al. 2021). This discrepancy arises from differences in methods, where our vorticity-based approach detected a larger number of systems, leading to a relatively smaller frequency of deep COLs. However, vorticity-based identification offers advantages over geopotential data as it avoids subjective threshold adjustments across pressure levels and is more sensitive to weaker COLs, providing a more consistent method for analyzing their vertical structure.

505 Further, we investigated the contrasting characteristics of COLs based on their vertical depth and intensity, categorizing them into four main types: shallow, deep, weak, and strong. Deep and strong COLs exhibit similar distribution patterns, predominantly concentrated in Australia and the southwestern Pacific. They are more intense and frequently found poleward of the subtropical jet, displaying a semi-annual oscillation peaking in autumn and spring. In contrast, shallow and weak COLs are less intense, situated more equatorward and with increased frequencies in summer. Our findings show the  
510 existence of a direct link between upper-tropospheric intensity and vertical depth of COLs, underscoring the significance of these classifications in understanding these atmospheric phenomena.

515 A particular novel aspect is the distinct role of the polar front and subtropical jets on different COL types. Deep COLs are significantly affected by the polar front jet, with a positive correlation observed between their occurrence and the jet intensity. This means a stronger polar front jet tends to lead to more frequent deep COLs, although no significant correlation was found regarding COL intensity. Conversely, shallow COLs show a significant negative correlation with the subtropical jet, indicating that their occurrences decrease with the jet intensification. Understanding these differential jet-COL interactions is crucial for comprehension of atmospheric dynamics, improving weather forecasting accuracy.

520 Unlike shallow systems, which weaken gradually towards the surface, deep COLs exhibit a multi-level vortex structure interconnected across different levels. Our findings suggest that the deep structure arises from an eddy feedback mechanism in some COLs due to the interaction between upper- and lower-tropospheric eddies. This feedback mechanism is initiated by a stronger upstream poleward jet, which induces more significant ageostrophic fluxes into the rear side of the COL system. Moreover, this process is accompanied by enhanced baroclinic conversion occurring west and east of the COLs. These stronger baroclinic processes and ageostrophic fluxes contribute to longer lifetimes and greater interaction between mechanisms operating at different levels within deep COL systems.

525 In this study, we have investigated the underlying mechanisms driving the deepening of COLs in the Southern Hemisphere, focusing on the regional variations in COL depths. Our analysis has also shed light on the impacts of diabatic processes on residual energy and its influence on the deepening of COLs.

530 Firstly, the sensitivity analysis of the track matching algorithm revealed that the estimation of COL depth is more responsive to changes in temporal overlap ( $\chi$ ) than the mean separation distance ( $d_m$ ) between tracks at different pressure levels. By adopting a small  $\chi$  value, we ensured the capture of the critical time steps during the life cycle of well defined stacked cyclonic systems. This approach identified 20% of COLs extending all the way to the surface, highlighting interconnected cyclonic features across various pressure levels. It is worth noting that the proportion of deep depth systems obtained using this approach is significantly lower than what were observed in previous studies (Poreù et al. 2007, Barnes et al. 2021). This disparity can be attributed to differences in methodologies between these studies as using vorticity a larger number of

535 systems are identified so the proportion is relative to a larger sample size. By adopting vorticity as the tracking variable, we avoid arbitrary decision in selecting thresholds for multiple levels, as can occur with geopotential. We believe that employing vorticity provides greater consistency in identifying cyclonic features, resulting in a more reliable assessment of their depths and behavior.

540 Regional differences in COL depths were then explored across eight genesis maxima regions in the Southern Hemisphere. Remarkably, deep COLs were found to be more frequent in regions E, F (southeast Australia), and H (southwest Atlantic Ocean), with approximately 30% of COLs extending all the way to the surface. These findings are consistent with earlier studies (Lim and Simmonds 2007, Barnes et al. 2021). Baroclinic conversion emerged as a significant mechanism contributing to the deepening of COLs in these regions, as also found in strong COLs (Pinheiro et al. 2022). In contrast, regions such as southeast Africa and the South Indian Ocean were characterized by predominantly shallow and medium-

545 depth systems. One contributing factor could be the intensified jet stream and baroclinicity observed over the South Atlantic and Indian oceans (Nakamura and Shimpø 2004). Notably, region G (southeast Pacific Ocean) showed a sharp decrease in COL extensions below 800 hPa. In this particular region, the development of COLs was observed to be influenced by upper-level ageostrophic fluxes, likely associated with stationary Rossby waves induced by the Andes Cordillera.

We categorized COLs into three groups based on their vertical extent: shallow, medium, and deep. Our analysis demonstrated considerable regional variations in the distribution of COLs across these categories. We particularly noted a latitude-dependent distribution, with deep COLs being more common at higher latitudes and less frequent north of 30°S. An interesting exception was observed in the southeastern Pacific, where deep and strong COLs tend to occur more frequently at lower latitudes compared to other regions.

From an energetics perspective, the comparison between shallow and deep COLs offered valuable insights into their vertical extent and deepening mechanisms. Deep COLs exhibited more vigorous energy growth due to stronger ageostrophic fluxes and enhanced baroclinic conversion. The presence of a more intense mid-latitude jet played a significant role in deepening COLs. These stronger baroclinic processes and ageostrophic fluxes contributed to longer lifetimes and greater interaction between mechanisms operating at different levels within the deep COL systems.

Shallow COLs showed a gradual weakening toward the surface, characterized by an anticyclonic circulation pattern. Conversely, deep COLs exhibited a distinct multi-level interconnected vortex structure. The presence of warm ascent air and mid-tropospheric diabatic heating contributed to the increase in eddy available potential energy that can be converted into eddy kinetic energy, leading to the coupling between upper and lower level depressions in deep COLs.

We further examined the impacts of A particular issue in our study is the misrepresentation of diabatic processes in reanalysis, including radiation and latent heating, on as they affect the residual energy and their potential possibly influence in the deepening of COLs. Negative residual energy dominated throughout the lifecycle of both shallow and deep COLs lifecycles, with deep COLs exhibiting significantly notably higher magnitudes in deep systems. The presence of negative (positive) residual energy to the east (west) of the COLs pointed points to the existence of dissipation (intensification) mechanisms not adequately represented in the reanalysis data, particularly possibly related to latent heating (radiative cooling), as discussed observed in Cavallo and Hakim (2010). Addressing the accurate representation of Accurately representing diabatic processes in reanalyses is essential to maintain consistency in the energetic analysis and emphasizes the need to investigate their influence for the understand their role in deepening of COLs. Therefore, it is crucial to re-evaluate COLs and the EKE budget whenever new reanalysis products such as ERA5 become available in future work.

In summary, this paper has significantly advanced our understanding of COL vertical extent in the Southern Hemisphere, providing valuable insights into their sensitivity, regional variations, and energetics. Future research can build on these findings to improve weather predictions and better prepare for the impacts of COLs on regional and global weather patterns.

In summary, our research highlights the significance of vertical depth and intensity in understanding key features of COLs, uncovering important associations between their diverse types and jet streams. However, further development of the energetic framework is necessary to incorporate vertical ageostrophic fluxes, as addressed in Rivière et al. (2015), potentially crucial for fully elucidating the eddy feedback mechanisms.

580 [Our research emphasizes the importance in classifying COL for understanding their key features and reveals their intricate relationships with jet streams. However, further development of the energetic framework, incorporating vertical ageostrophic fluxes as in Rivière et al. \(2015\), remains essential for comprehensively elucidating the eddy feedback mechanisms.](#)

### Acknowledgements

We would like to thank CNPq (Conselho Nacional de Desenvolvimento Científico e Tecnológico, Grant: 151225/2023-0) and FAPESP (Fundação de Amparo à Pesquisa do Estado de São Paulo, Grant: 2023/10882-2) for their support and funding throughout this research. The authors have employed artificial intelligence (AI) to enhance the quality of the paper's writing.

### References

[Bals-Elsholz, T. M., Atallah, E. H., Bosart, L. F., Wasula, T. A., Cempa, M. J., and Lupo, A. R.: The wintertime Southern Hemisphere split jet: Structure, variability, and evolution. \*Journal of climate\*, 14, 4191–4215, 2001.](#)

590 Barnes, M. A., Ndarana T., and Landman, W. A.: Cut-off lows in the Southern Hemisphere and their extension to the surface, *Climate Dynamics*, 56, 3709–3732, doi:10.1007/s00382-021-05662-7, 2021.

Bengtsson, L., Hodges, K. I., and Keenlyside, N.: Will extratropical storms intensify in a warmer climate?, *Journal of Climate*, 22, 2276–2301, doi:10.1175/2008JCLI2678.1, 2009.

[Catto, J. L.: A new method to objectively classify extratropical cyclones for climate studies: Testing in the southwest Pacific region. \*Journal of Climate\*, 31, 4683–4704, doi:10.1175/JCLI-D-17-0746.1, 2018.](#)

600 Cavallo, S. M. and Hakim, G. J.: Composite structure of tropopause polar cyclones, *Monthly Weather Review*, 138, 3840–3857, doi:10.1175/2010MWR3371.1, 2010.

[Chang, E. K.: Wave packets and life cycles of troughs in the upper troposphere: Examples from the Southern Hemisphere summer season of 1984/85. \*Monthly Weather Review\*, 128, 25–50, doi: 10.1175/1520-0493\(2000\)128<0025:WPALCO>2.0.CO;2, 2000](#)

Davis, C. A. and Emanuel, K. A.: Potential vorticity diagnostics of cyclogenesis, *Monthly Weather Review*, 119, 1929–1953, doi:10.1175/1520-0493(1991)119<1929:PVDOC>2.0.CO;2, 1991.

[Danielson, R. E., Gyakum, J. R., Straub, D. N.: A case study of downstream baroclinic development over the North Pacific Ocean. Part II: Diagnoses of eddy energy and wave activity. \*Monthly weather review\*, 134, 1549–1567, doi:10.1175/MWR3173.1, 2006](#)

605 Dee, D. P., et al.: The ERA-Interim reanalysis: configuration and performance of the data assimilation system, *Quarterly Journal of the Royal Meteorological Society*, 137, 553–597, doi:10.1002/qj.828, 2011.

[Favre, A., Hewitson, B., Tadross, M., Lennard, C., Cerezo-Mota, R.: Relationships between cut-off lows and the semiannual](#)

[and southern oscillations. \*Climate dynamics\*, 38, 1473–1487, doi:10.1007/s00382-011-1030-4, 2012](#)

610 Frank, N. L.: On the energetics of cold lows. In: Symposium on tropical meteorology. Proceedings... American Meteorological Society EIV1-EIV6, 1970.

[Deser, C. et al.: The effects of North Atlantic SST and sea ice anomalies on the winter circulation in CCM3. Part II: Direct and indirect components of the response. \*Journal of Climate\*, 17, 5, 877–889, doi:10.1175/1520-0442\(2004\)017<0877:TEONAS>2.0.CO;2, 2004.](#)

615 Gan, M. A. and Dal Piva, E.: Energetics of a southeastern Pacific cut-off low, *Atmospheric Science Letters*, 14, 272–280, doi:10.1002/asl2.451, 2013.

Gan, M. A. and Dal Piva, E.: Energetics of southeastern Pacific cut-off lows, *Climate Dynamics*, 46, 3453–3462, doi:10.1007/s00382-015-2779-7, 2016.

620 Garreaud, R. D. and Fuenzalida, H. A.: The influence of the Andes on cutoff lows: a modeling study, *Monthly Weather Review*, 135, 1596–1613, doi:10.1175/MWR3350.1, 2007.

[Hodges, K. I.: A general method for tracking analysis and its application to meteorological data, \*American Meteorological Society\*, 122, 2573–2585, doi:10.1175/1520-0493\(1994\)122<2573:AGMFTA>2.0.CO;2, 1994.](#)

[Hodges, K. I. Feature tracking on the unit sphere. \*Monthly Weather Review\*, 123, 3458–3465, doi:10.1175/1520-0493\(1995\)123<3458:FTOTUS>2.0.CO;2, 1995.](#)

625 Hodges, K. I.: Spherical nonparametric estimators applied to the UGAMP model integration for AMIP, *Monthly Weather Review*, 124, 2914–2932, doi:10.1175/1520-0493(1996)124<2914:SNEATT>2.0.CO;2, 1996.

Hodges, K. I.: Adaptive constraints for feature tracking, *Monthly Weather Review*, 127, 1362–1373, doi:10.1175/1520-0493(1999)127<1362:ACFFT>2.0.CO;2, 1999.

630 Hodges, K. I., Boyle, J., Hoskins, B. J., and Thorncroft, C.: A comparison of recent reanalysis datasets using objective feature tracking: storm tracks and tropical easterly waves, *Monthly Weather Review*, 131, 2012–2037, doi:10.1175/1520-0493(2003)131<2012:ACORRD>2.0.CO;2, 2003.

Hodges, K. I., Lee, R. W., and Bengtsson, L.: A comparison of extratropical cyclones in recent reanalyses ERAI, NASA MERRA, NCEP CFSR, and JRA-25, *Journal of Climate*, 24, 4888–4906, doi:10.1175/2011JCLI4097.1, 2011.

635 Hodges, K., Cobb, A., Vidale, P. L., Hodges, K., Cobb, A., and Vidale, P. L.: How well are tropical cyclones represented in reanalysis datasets?, *Journal of Climate*, 30, 5243–5264, doi:10.1175/JCLI-D-16-0557.1, 2017.

[Hoskins, B. J., Karoly, D. J.: The steady linear response of a spherical atmosphere to thermal and orographic forcing. \*Journal of the atmospheric sciences\*, 38, 1179–1196, doi:10.1175/1520-0469\(1981\)038<1179:TSLROA>2.0.CO;2, 1981](#)

- [Kushner, P. J., Held, I. M., Delworth, T. L.: Southern Hemisphere atmospheric circulation response to global warming. \*Journal of Climate\*, 14, 2238–2249, doi:10.1175/1520-0442\(2001\)014<0001:SHACRT>2.0.CO;2, 2001](#)
- 640 [Lakkis, S. G., Canziani, P., Yucechen, A., Rocamora, L., Caferri, A., Hodges, K., O'Neill, A. A 4D feature-tracking algorithm: a multidimensional view of cyclone systems. \*Quarterly Journal of the Royal Meteorological Society\*, 145, 395–417, doi:10.1002/qj.3436, 2019.](#)
- [Lim, E. P., Simmonds, I.: Southern Hemisphere winter extratropical cyclone characteristics and vertical organization observed with the ERA-40 data in 1979–2001. \*Journal of Climate\*, 20, 2675–2690, doi:10.1175/JCLI4135.1, 2007.](#)
- 645 [Llasat, M. C., Martín, F., and Barrera, A.: From the concept of “Kaltlufttropfen”\(cold air pool\) to the cut-off low. The case of September 1971 in Spain as an example of their role in heavy rainfalls, \*Meteorology and Atmospheric physics\*, 96, 43-60, doi:10.1175/JCLI-D-16-0557.1, 2007.](#)
- [Lu, J., Sun, L., Wu, Y., Chen, G.: The role of subtropical irreversible PV mixing in the zonal mean circulation response to global warming–like thermal forcing. \*Journal of Climate\*, 27, 2297–2316, doi:10.1175/JCLI-D-13-00372.1, 2014](#)
- 650 [Marshall G. J.: Trends in the Southern Annular Mode from observations and reanalyses. \*Journal of Climate\*, 16: 4134–4143.](#)
- [McInnes, K. L. and Hubbert, G. D.: The impact of eastern Australian cut-off lows on coastal sea levels, \*Meteorol. Appl.\*, 8, 229–244, doi:10.1017/S1350482701002110, 2001.](#)
- [Nakamura, H.: Midwinter suppression of baroclinic wave activity in the Pacific. \*Journal of Atmospheric Sciences\*, 49, 1629–1642, doi.org/10.1175/1520-0469\(1992\)049<1629:MSOBWA>2.0.CO;2, 1992.](#)
- 655 [Nakamura, H. and Shimpo, A.: Seasonal variations in the Southern Hemisphere storm tracks and jet streams as revealed in a reanalysis dataset, \*Journal of Climate\*, 17, 1828–1844, doi:10.1175/1520-0442\(2004\)017<1828:SVITSH>2.0.CO;2, 2004.](#)
- [Ndarana, T. and Waugh, D. W.: The link between cut-off lows and Rossby wave breaking in the Southern Hemisphere. \*Quarterly Journal of the Royal Meteorological Society\*, 136, 869–885, 2010.](#)
- [Ndarana, T., Rammopo, T. S., Chikoore, H., Barnes, M. A., and Bopape, M. J.: A quasi-geostrophic diagnosis of the zonal flow associated with cut-off lows over South Africa and surrounding oceans, \*Climate Dynamics\*, 55, 2631–2644, doi:10.1007/s00382-020-05401-4, 2020.](#)
- 660 [Ndarana, T., Rammopo, T. S., Bopape, M. J., Reason, C. J., and Chikoore, H.: Downstream development during South African cut-off low pressure systems, \*Atmospheric Research\*, 249, 105315, doi:10.1016/j.atmosres.2020.105315, 2021.](#)
- [Nieto, R., et al.: Climatological features of cutoff low systems in the Northern Hemisphere, \*Journal of Climate\*, 18, 3085–3103, doi:10.1175/JCLI3386.1, 2005.](#)
- 665

- Orlanski, I., Katzfey, J.: The life cycle of a cyclone wave in the Southern Hemisphere: eddy energy budget, *Journal of the Atmospheric Sciences*, 48, 1972–1998, doi:10.1175/1520-0469(1991)048<1972:TLCOAC>2.0.CO;2, 1991.
- Palmén, E.: Origin and structure of high-level cyclones south of the maximum westerlies, *Tellus*, 1, 22–31, doi:10.1111/j.2153-3490.1949.tb01925.x, 1949.
- 670 ~~[Pinto, J. R. D. and da Rocha, R. P.: The energy cycle and structural evolution of cyclones over southeastern South America in three case studies, \*Journal of Geophysical Research\*, 116, 1–17, doi:10.1029/2011JD016217, 2011.](#)~~
- Pinheiro, H. R., Hodges, K. I., Gan, M. A., and Ferreira, N. J.: A new perspective of the climatological features of upper-level cut-off lows in the Southern Hemisphere, *Climate Dynamics*, 48, 541–559, doi:10.1007/s00382-016-3093-8, 2017.
- Pinheiro, H. R., Hodges, K. I., and Gan, M. A.: Sensitivity of identifying Cut-off Lows in the Southern Hemisphere using multiple criteria: implications for numbers, seasonality and intensity, *Climate Dynamics*, 53, 6699–6713, doi:10.1007/s00382-019-04984-x, 2019.
- 675 Pinheiro, H. R., Hodges, K. I., and Gan, M. A.: An intercomparison of Cut-off Lows in the subtropical Southern Hemisphere using recent reanalyses: ERA-Interim, NCEP-CFSR, MERRA-2, JRA-55, and JRA-25, *Climate Dynamics*, 54, 777–792, doi:10.1007/s00382-019-05089-1, 2020.
- 680 Pinheiro, H. R., Gan, M. A., and Hodges, K. I.: Structure and evolution of intense austral Cut-off Lows, *Quarterly Journal of the Royal Meteorological Society*, 147, 1–20, doi:10.1002/qj.3900, 2021.
- Pinheiro, H. R., Hodges, K. I., Gan, M. A., Ferreira, S. H., and Andrade, K. M.: Contributions of downstream baroclinic development to strong Southern Hemisphere cut-off lows, *Quarterly Journal of the Royal Meteorological Society*, 148, 214–232, doi:10.1002/qj.4201, 2022.
- 685 ~~[Pinto, J. R. D. and da Rocha, R. P.: The energy cycle and structural evolution of cyclones over southeastern South America in three case studies, \*Journal of Geophysical Research\*, 116, 1–17, doi:10.1029/2011JD016217, 2011.](#)~~
- Porcù, F., Carrassi, A., Medaglia, C. M., Prodi, E., and Mugnai, A.: A study on cut-off low vertical structure and precipitation in the Mediterranean region, *Meteorology and Atmospheric Physics*, 96, 121–140, doi:10.1007/s00703-006-0224-5, 2007.
- 690 Portmann, R., Crezee, B., Quinting, J., and Wernli, H.: The complex life cycles of two long-lived potential vorticity cut-offs over Europe, *Quarterly Journal of the Royal Meteorological Society*, 144, 701–719, doi:10.1002/qj.3239, 2018.
- ~~[Portmann, R., Sprenger, M., & Wernli, H.: The three-dimensional life cycle of potential vorticity cutoffs: a global and selected regional climatologies in ERA-interim \(1979–2018\). \*Weather and Climate Dynamics\*, 2, 1–52, doi:10.5194/wcd-2-507-2021, 2021.](#)~~

695 [Rivière, G., Arbogast, P., Joly, A. Eddy kinetic energy redistribution within windstorms Klaus and Friedhelm. Quarterly Journal of the Royal Meteorological Society, 141, 925–938, doi:10.1002/qj.2412, 2015.](#)

Sakamoto, K. and Takahashi, M.: Cut off and weakening processes of an upper cold low, Journal of the Meteorological Society of Japan, 83, 817–834, doi:10.2151/jmsj.83.817, 2005.

700 [Simmonds, I. and Jones, D. A.: The mean structure and temporal variability of the semiannual oscillation in the southern extratropics. International Journal of Climatology: A Journal of the Royal Meteorological Society, 18, 473–504, 1998.](#)

[Sinclair, M. R., Revell, M. J: Classification and composite diagnosis of extratropical cyclogenesis events in the southwest Pacific. Monthly Weather Review, 128, 1089–1105, doi:10.1175/1520-0493\(2000\)128<1089:CACDOE>2.0.CO;2, 2000.](#)

Singleton, A. T. and Reason, C. J. C.: A numerical model study of an intense cutoff low pressure system over South Africa, Monthly weather review, 135, 1128–1150, doi:10.1175/MWR3311.1, 2007.

705 [Stoelinga, M. T.: A potential vorticity-based study of the role of diabatic heating and friction in a numerically simulated baroclinic cyclone, Monthly Weather Review, 124, 849–874, doi:10.1175/1520-0493\(1996\)124<0849:APVBSO>2.0.CO;2, 1996.](#)

[Trenberth, K. E.: Storm tracks in the Southern Hemisphere. Journal of Atmospheric Sciences, 48, 2159–2178, doi:10.1175/1520-0469\(1991\)048<2159:STITSH>2.0.CO;2, 1991.](#)

710 [Van Loon, H.: The half-yearly oscillations in middle and high southern latitudes and the coreless winter. Journal of Atmospheric Sciences, 24, 472–486, 1967.](#)

~~[Vuille, M. and Ammann, C.: Regional snowfall patterns in the high, arid Andes, Climatic change, 36, 413–423, doi:10.1023/A:1005330802974, 1997.](#)~~

715

720

## Appendix

725 See Table A.1.

**Table A.1** Sensitivity of the number of  $\xi_{300}$  COLs to time overlap for each pressure level (hPa), expressed as a percentage of the total number. The overlap thresholds are 1%, 5%, 10%, 25%, 50%, 75%, and 100%.

	1%	5%	10%	25%	50%	75%	100%
300	100.0	100.0	100.0	100.0	100.0	100.0	100.0
400	80.9	80.9	80.9	80.8	79.2	66.0	11.2
500	65.5	65.5	65.5	65.1	61.9	42.9	2.2
600	51.1	51.0	50.9	50.3	45.7	25.8	0.5
700	37.7	37.7	37.5	36.9	31.6	14.9	0.2
800	28.8	28.8	28.6	28.0	23.0	9.7	0.1
900	23.1	23.0	22.9	22.3	18.1	6.9	0.0
1000	20.3	20.2	20.1	19.5	15.4	5.6	0.0

### 730 Code/data availability

The code used in this study is available upon request from the corresponding author for researchers interested in reproducing or extending the findings presented in the paper. The ERA-Interim reanalysis data was sourced from the ECMWF server. Please contact corresponding author's email for access to the code.

### Author Contributions

735 Henri Pinheiro: Conceptualization, investigation, data curation, methodology, writing – original draft, visualization.

Kevin Hodges: Software development, writing - review and editing.

Manoel Gan: Writing - review and editing.

### Competing interests

The authors declare no competing interests in relation to the research, authorship, or publication of this paper.